Cyclicity and stability of grey-sided voles, *Clethrionomys rufocanus*, of Hokkaido: spectral and principal components analyses

OTTAR N. BJØRNSTAD[1], STEPHANE CHAMPELY[2],
NILS CHR. STENSETH[1]* AND TAKASHI SAITOH[3]

[1]*Division of Zoology, Department of Biology, University of Oslo, P.O. Box 1050, Blindern, N-0316 Oslo, Norway*
[2]*IUT STID, Ile du Saulcy, 57045 METZ cedex 1, France*
[3]*Hokkaido Research Centre, Forestry and Forest Products Research Institute, Hitsujigaoka 7, Toyohira, Sapporo, Japan 062*

SUMMARY

A spatio-temporal data panel of abundances of the grey-sided vole of Hokkaido (Japan) is analysed. The data consist of annual censuses of 90 populations from 1962–1992. The region studied covers approximately 160×220 km. The 90 time series spanning 31 years are analysed using a combination of spectral analysis, principal components analysis and graphical methods. Through this we demonstrate that vole populations in the northwestern coastal region of Hokkaido exhibit seasonal population dynamics, whereas those in the more mountainous northeastern and central regions exhibit multiannual cycles. The multiannual cycles have a period of 3.5–4 years. The findings are related to other studies from Hokkaido as well as studies of North European microtines.

1. INTRODUCTION

Microtine rodents supply some of the best examples on how the population dynamics of a species can change on a biogeographic scale (Henttonen *et al.* 1985). Best known is the dynamics of the microtine populations in Fennoscandia (see, for example, Stenseth & Ims 1993): southern populations do not exhibit regular multi-annual fluctuations (Hansson 1971), whereas northern populations of the same species exhibit dramatic cycles (e.g. Hansson & Henttonen 1985). Within the cyclic region, both cycle length and amplitude increase with altitude (e.g. Hanski *et al.* 1991; Bjørnstad *et al.* 1995). On a larger scale, the differences may also be conspicuous. The abundance of muskrat (*Ondatra zibethica*), for instance, undergo regular fluctuations with a period of 10 years in North America (e.g. Elton & Nicholson 1942; Bulmer 1974), but with a period of approximately 4 years in Sweden (Danell 1985). The northern red-backed vole (*Clethrionomys rutilus*) is an example of a species which exhibit 4 year cycles in Fennoscandia, but appear to be non-cyclic in North America (Henttonen *et al.* 1985; Gilbert & Krebs 1991). Differences like these, either in the form of clinal gradients or in the form of sharp boundaries, are important when trying to disentangle what determines the dynamics of populations. Such geographic patterns permit a comparative approach to the study of population dynamics. Consequently, detailed description of the geographic patterns is important.

Here we study a panel of time series of the grey-sided vole (*Clethrionomys rufocanus*; Sundevall 1846) from the Japanese island of Hokkaido. We demonstrate regional differences in population dynamics across an area of approximately 160×220 km. We also illustrate how multivariate statistics can aid in the understanding of spatio-temporal panels of abundance data.

2. MATERIAL AND METHODS

Evidence of geographic gradients arise from comparisons of time series of abundance indices. Such spatio-temporal panels of data pose challenging methodological problems in the interface between time series analysis (e.g. Priestley 1981; Wei 1989) and spatial statistics (e.g. Upton & Fingleton 1985). Usually this is resolved by collapsing the temporal dimension of the data to one or a few time-independent descriptors. Examples of such time independent descriptors are: the dominant period of the periodogram (e.g. Henttonen *et al.* 1985; Hanski *et al.* 1991); indices of variability (e.g. Hansson & Henttonen 1985; Henttonen *et al.* 1985; Hanski *et al.* 1994); and coefficients of direct and delayed statistical density dependence (Bjørnstad *et al.* 1995). The uni-dimensional descriptors are subsequently subjected to classical univariate analysis. However, in the process of eliminating the temporal dimension of the data, much information is lost. By using multivariate ordination techniques, it is possible to optimize this reduction and to minimize the amount of information discarded. As will be clear, this approach may enhance the power of the study greatly.

* Author to whom correspondence should be addressed.

(a) The study area

Hokkaido is the northern-most island of Japan, it has a mountainous interior in the North levelling off towards the planes along the coast. The island has snowy cold winters and warm humid summers (Saitoh 1987; Henttonen *et al.* 1992). The duration of the snow cover is around 4 months, and the snow depth may reach as much as 1 m. Voles from the northern area of Hokkaido is considered in this study (see figure 2). Within this region, the east coast and interior is colder than the west. Hence, the duration of the snowy season is longer in the eastern mountainous region (130–140 days snow > 10 cm) than in the western coastal region (110–120 days snow > 10 cm), and the maximum snow depth is found in the northeast.

The natural vegetation of the study area belong to the mixed forest type consisting of broad-leaved and coniferous trees (Tatewaki 1958). The relative proportion of the these trees vary from area to area. Generally the proportion of coniferous tree increase with altitude and latitude. There are, however, no major vegetational boundaries going through the study area (Tatewaki 1958). Within the area studied, all forests but the most eastern are situated below an altitude of 1000 m. From this highland area, the altitude decreases gradually northwards and westwards. All but the extreme most northwestern forests are situated above 100 m.

(b) The data

The grey-sided vole (*C. rufocanus*) is the most abundant vole species on Hokkaido (Saitoh 1987). It inhabits indigenous forest as well as forest plantations. The populations may reach pest-like densities in some years, causing severe economic damage to the forest industry (Saitoh 1987). In the wild it exhibits many common microtine life-history characteristics. Females are territorial with density-dependent maturation rates and home-range size (Saitoh 1991). The main reproductive period is from April/May to September/October, but some subnivean reproduction has been recorded during the winter (Nakata 1989). The data analysed in this study is from a census at the end of the reproductive period (below), where the densities are expected to be at their yearly maximum (Nakata 1989).

At least four muride species are sympatric to the grey-sided vole. These are the two microtines *C. rutilus* and *C. rex* (the latter is now considered synonymous with *C. rufocanus*; Wilson & Reeder 1993), and the two murines *Apodemus speciosus* and *A. argenteus*. These species are all numerically inferior to *C. rufocanus* in the forest habitat. Several vole predators are found on Hokkaido (Henttonen *et al.* 1992; Dobson 1994). Three species of mustelid: *Mustela nivalis*, *M. sibirica* (syn.: *M. itatsi*), and *M. vison* are specialist vole predators. In addition, some generalist predators such as foxes and various predatory birds include voles as an important part of their diet (Henttonen *et al.* 1992).

The material investigated here is a subset of the data collected by the Japan Forest Agency over a period of 31 years (1962–1992). A standardized census trapping of the small rodent community was carried out three times a year. Each ranger office of Hokkaido carried out at least two parallel trappings; one in natural forest habitat and one in planted forest habitat. Pesticides were periodically applied to the plantations and so these data are not considered further here. Each trapping session consisted of 250 trap nights in the period 1962–1976 and 150 trap nights thereafter. The data from the first part was transformed into 150 night equivalents using the empirical relation (determined on a subset of the data where detailed information is available): $y = 0.68x + 0.18$ ($R^2 = 0.97$; where x is the 250 night trap count, and y is the 150 night equivalent) for all but zero abundances (see Saitoh *et al.* 1996). This rescaling will incur some additional uncertainty. We have, however, no reason to believe that conclusions drawn are affected in any major way by this.

The trapping area covered 0.5 ha in all years. There are 436 ranger offices involved in the rodent censusing on Hokkaido. Of these 151 reside in the northern area considered here. We analyse the time series of autumn (Sept/Oct) censuses in natural forest from these.

Due to methodological limitations, we only investigate the series for which no values are missing. This subset of the data consists of 90 time series. The raw data, thus, constitute a panel of data with 90 spatial and 31 temporal locations. The median distance to the nearest neighbouring census point is 8 km (range: 3.3–27.8). A part of the data has been analysed previously by Saitoh *et al.* (1987). Saitoh *et al.* (1996) provide a full description of the structure of the Japanese Forestry Agency and the compilation of the data.

(c) Statistical analysis

The number of voles in a population are generally governed by birth and death processes. Such processes operate in a multiplicative, rather than an additive, fashion. A logarithmic scale (natural logarithm) is therefore a natural scale on which to consider the observations (e.g. Royama 1992; Bjørnstad *et al.* 1995). Due to the occurrence of zero observations, a constant of unity was added to all observations before log-transformation. Methods for the analyses of time series generally assume stationarity (time independence of the mean, variance and covariance of the series; Priestly 1981). Approximate stationarity is commonly obtained by differencing the series (Priestley 1981). Biologically speaking this amounts to analysing the sequence of growth rates, rather than the sequence of log-abundances (Royama 1992). Although our time series generally appear stationary, we nevertheless carried out the analyses on the growth rates, to ensure that none of the results are due to violations of this assumption. The sequence of growth rates will have several properties which are different from the sequence of original observations. However, the qualitative periodic behaviour will be the same.
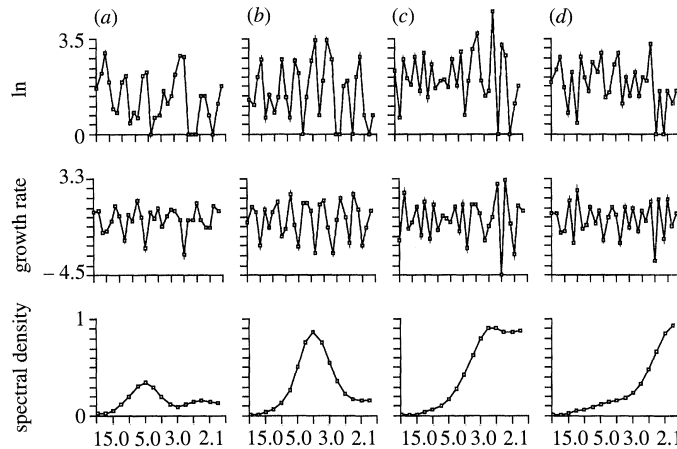
Figure 1. The four time series constituting our main examples. The top row (ln) depicts the log transformed abundances. The second row depicts the sequence of growth rate (the 1st difference of the log abundances). The bottom row depicts the spectral densities. The spectral densities are estimated from the time series of growth rates using a Parzen window (width 5). (*a*) Multiannual fluctuations which are relatively irregular (population no. 75). (*b*) Multiannual and regular fluctuations (population no. 9). (*c*) Largely biannual oscillations but with indication of some longer rhythms (population no. 43). (*d*) Biannual oscillation: dominance of the highest frequency (population no. 88).

Some of the time series can, by visual inspection, be seen to entertain multiannual cycles. They have dynamics resembling the classical 'microtine cycles' (see, for example, Stenseth & Ims 1993). Figure 1 depicts four time series (log transformed data), and their accompanying growth rates and spectral densities (estimated using a Parzen window; see below). These four series span the range of variation in population periodicities observed in the data, from multiannual cyclic to biannual or possibly seasonal dynamics (cf. cyclic versus 'semi-stable' dynamics; Hansson & Henttonen 1985). Notice how the spectral profiles of the series shift gradually from figure 1*a–d*. These four time series are used as illustrations throughout the text. The dominant peak of the estimated spectral densities of the 90 time series are plotted at their spatial coordinates in figure 2. The geographic pattern – if any – is not pronounced in this univariate summary statistic.

Principal Components Analysis (PCA; see for example, Jackson 1986) is a commonly used method for extracting the main features of high-dimensional data. This technique is, however, most powerful in summarizing smooth patterns in time series, such as trends through time (see Colebrook 1978). The main characteristic of the present time series is high frequency oscillations and not trends (figure 1). Hence, it is of interest to analyse the series in the frequency domain: that is, to examine the spectral densities. Changes in oscillatory behaviour (cyclicity) may appear as smooth transitions of frequencies.

In a spectral decomposition, each time series is transformed into a sum of sine and cosine functions of different period lengths (e.g. Wei 1989):

$$x_t = \sum_{k=0}^{p/2} [a_k \cos(2\pi kt/p) + b_k \sin(2\pi kt/p)], \qquad (1)$$

where p is the length of the series, $\{2\pi kt/p\}_{k=0\ldots p/2}$ is the sequence of frequencies at which the spectrum is estimated, and a_k and b_k are the Fourier coefficients. When $k \neq 0$, the Fourier coefficients capture the different rhythms in the data. The mean is captured by the coefficient a_0. The importance of each frequency (rhythm), k, is given by its coefficient a_k and b_k as:

$$R_k = \begin{cases} \dfrac{n}{2}(a_k^2 + b_k^2) & k = 1, \ldots, (p-1)/2 \\ n\,(a_k^2) & k = 0 \quad \text{and} \quad (p)/2 \end{cases}, \qquad (2)$$

where n is the number of observations. The sum of all these, ΣR_k, is equal to the total sum-of-squares of the time series. In this way the spectral decomposition is a transformation which retains the variability of the original data. The usual way of summarizing the decomposition of the time series is the periodogram: the graph of the R_k as a function of the frequency $2\pi kt/p$. Whenever desirable, the frequencies can be transformed into periods (period = 1/frequency).

The crude 'periodogram' based on equations 1 and 2 is an estimate of the 'spectral density' of the time series (just like the sample mean is an estimate of the population mean). The periodogram is, however, a poor estimator. It has very large variance and it is not statistically consistent (Priestley 1981). Several superior estimators have been developed. In this analysis we use a Parzen smoothing window to estimate the spectral density. We employ a window width of 5 as recommended for time series of length 30 (Priestley 1981). The underlying spectral density is a continuous function. The estimator gives a discrete version of this with 16 points for each time series. The discrete spectral densities of our time series thus generate a data matrix of 90 rows and 16 columns.

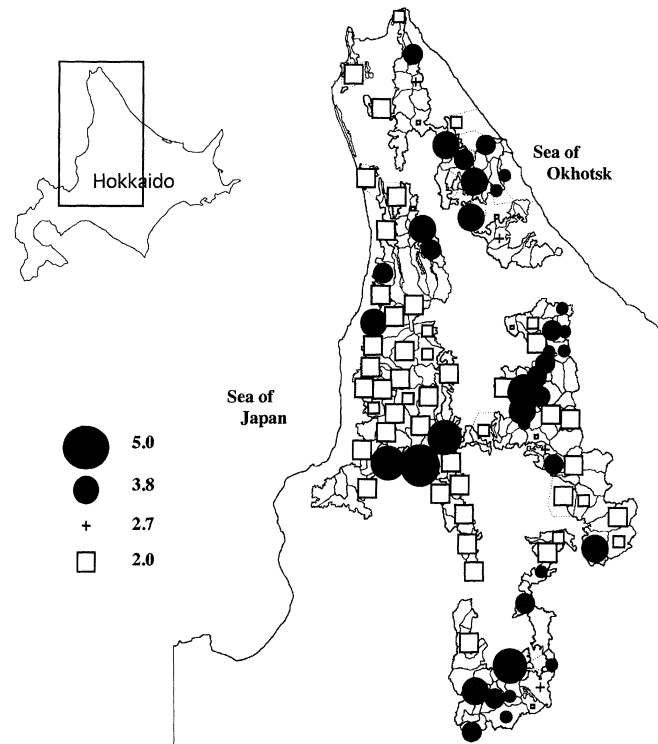The interpretation of the spectrum (amplitude against frequency graph) of a time series is that large

Figure 2. The dominant period (the peak spectral density) of the 90 populations plotted at their spatial coordinates. The lines mark the border between the different forest offices in this part of Hokkaido. Large open squares represent short periods, large filled circles represent long periods. The spectral densities are estimated from the time series of the growth rates of the populations (i.e. the first difference of the log-abundances) using a Parzen window (width 5).

amplitudes in the low frequency region (left) of the graph represent long term trends and rhythms (no examples in the present data; however, even if such trends did exist, they would vanish in the first differenced data). Large amplitudes in the high frequency region (right) of the graph (e.g. figure 1 *c* & *d*) represent two-year cycles. Large amplitudes in the central part of the spectrum signifies cyclic fluctuations (figure 1 *a* & *b*). The dominant frequencies of the time series in figure 1 *a* & *b* corresponds to 5 and 3.75 year cycles, respectively. Noisy or completely aperiodic dynamics give rise to a periodogram with no conspicuous maximum (see, for example, series 1 and 14 of figure 7).

PCA identifies the main features of the set of spectral densities through decomposing the multivariate table into a lower dimensional system using only the most important eigenvectors (e.g. Jackson 1986). Each spectral density (row) will be approximated by a linear combination of these eigenvectors. The aim of the analysis is to find a small number of eigenvectors to optimally (in a mean-square sense) describe the data. The coefficients in the linear combinations are called the row scores. These row scores can be summarized graphically as: (i) a classical factor map; (ii) a biplot (Gabriel 1971); or (iii) by plotting them on a map (whenever the data has been recorded at explicit spatial locations; Goodall 1954). The biplot is a factor

map (the scatter plot of the row scores), with the standardized column scores superimposed. In this way, it summarizes the decomposition more fully. To investigate the descriptive power and fit of the multivariate decomposition, data reconstitution (Eckart & Young 1936) is an important tool (Castro *et al.* 1986). The data are reconstituted (predicted) using the first few and most important eigenvectors. This may be carried out sequentially so that the contribution and effect of each principal component is visualized. The number of principal components needed to describe the data is determined by the magnitude of the eigenvalues (Jackson 1986). Small eigenvalues signify that the principal component explain very little of the variation in the data. Such a principal component is likely to be spurious or unimportant.

To elucidate the relation between the calculated row scores and two geographic quantities (altitude and distance from the Sea of Japan) a non-parametric (generalized additive) regression was employed (using a LOESS smoother of degree 2; Hastie & Tibshirani 1990).

Spectral analyses was performed using SAS version 6.08 (SAS Inst. 1990), Multivariate analyses and plotting was performed using ADE version 3.7 (Chessel & Dolédec 1992), and the non-parametric regression was performed using the GAM function of S-plus version 3.2 (Statistical Sciences 1993).

3. RESULTS

Performing PCA on the table of spectral densities facilitates a drastic reduction in the dimensionality of the data. The first two axes encompass 85 % of the variation in the spectral densities, and the first three as much as 95 %. It appears that two, or possibly three,
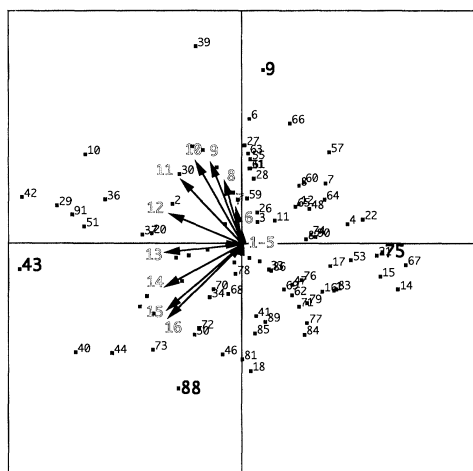
Figure 3. Biplot of the centred PCA of the table of spectral densities. The scatter plot is of the scores of the two principal eigenvectors. Each scatter point represent a unique time series. The four time series used as our main examples are indicated in bold face (nos. 75, 9, 43, and 88). Each arrow with associated contour text represents the standardized column scores of the spectral frequencies. The length of the arrow indicate the overall importance of this frequency in the ordination. The direction indicate how the frequency correlate with the principal components. The frequencies 1–6 are not very useful for discriminating the populations (the arrows have nearly no length). The second axis is positively correlated with the multiannual cyclic frequencies (7–10) and negatively correlated with the short term frequencies (14–16). The first axis is related to the overall average of each frequency ('the mean effect'). On the negative side the time series exhibit dominant frequencies in the inter-annual to multiannual cyclic frequencies, whereas on the positive side these frequencies are relatively unimportant.
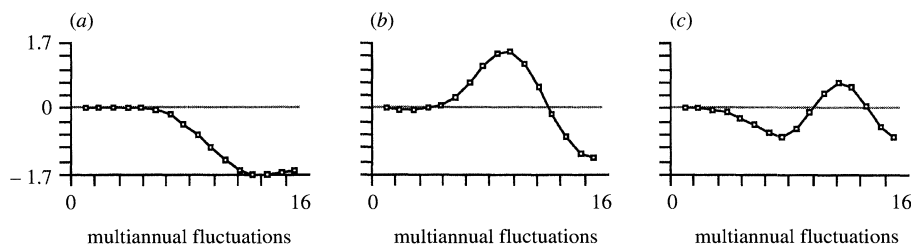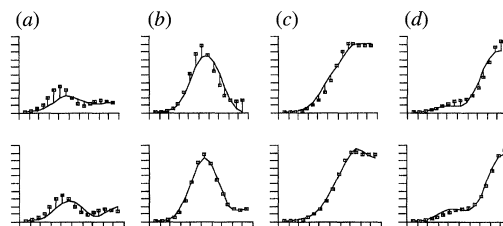
Figure 5. Reconstitution of the four main examples based on the first two and the first three eigenvectors. The small squares represent the actual spectral densities, the curve represent the reconstitution. The vertical lines visualize the discrepancy. Top row: 2 axes reconstitution; bottom row: 3 axes reconstitution.

eigenvectors are important. The biplot (figure 3) for the first two axes reveal the importance of columns 8 to 16. These columns represent fluctuations with periods from 4.3 to 2.0 years.

Two years is the shortest rhythm it is possible to observe, using spectral analysis, in annual censuses. There is little relation between columns 1–7 (representing frequencies with periods from 30 to 5.3 years) and any of the axes. The first axis represents oscillations in the high frequency end of the spectrum. In this way it encompasses both short-term rhythms and multiannual cycles. The second axis is positively linked with columns 7–11 (fluctuations with periods 5 to 3 years) and negatively linked with columns 14–16 (short term oscillations; periods 2.3 to 2.0 years). Hence, this second axis captures the dichotomy between conspicuously cyclic populations and annual or biannual dynamics (see below). Note, that the four time series used as our main examples (series 75, 9, 43 and 88) are at the extreme corners of the biplot. Thus, as stated above, they truly span the range of variation of oscillatory behaviour of the populations.

The meaning of the axes of the ordination is more clear when the eigenvectors are plotted as spectral densities (empirical orthogonal functions, Castro *et al.* 1986). Figure 4 depicts the three important eigenvectors. The first axis captures the general level of

Figure 4. The first 3 standardized eigenvectors plotted as periodograms. Long periods are at the left and short periods at the right of each graph. (*a*) The first eigenvector is the 'mean effect'. (*b*) The second eigenvector captures the cyclicity, it allows a description of the opposition between the annual/biannual dynamics and the multiannual cycles. (*c*) The third eigenvector is a modulator of the dominant period; the sum of (*b*) and (*c*) will give a periodogram with a peak at slightly shorter period (shifted to the right) than (*b*) alone. Note that the values for the high periods (right end of axis) is generally zero. This is linked to the indiscrimination of this part of the spectrum (see text and caption of figure 3).
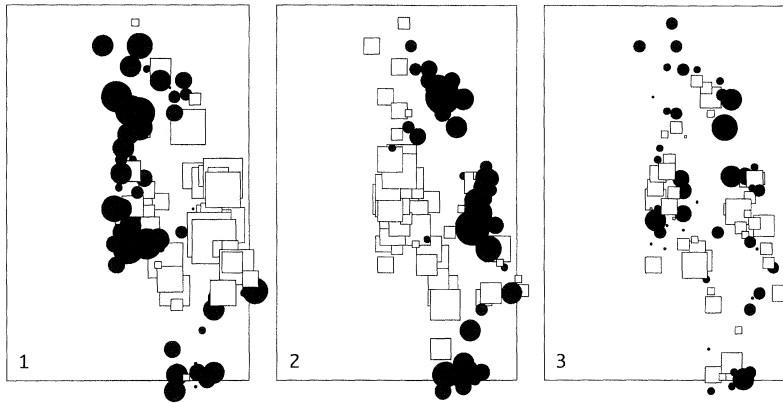
Figure 6. Spatial representation of the first three row scores. The size of the symbols are proportional to the absolute value of the score, black circles signifies positive values and white squares negative values (cf. figure 2).
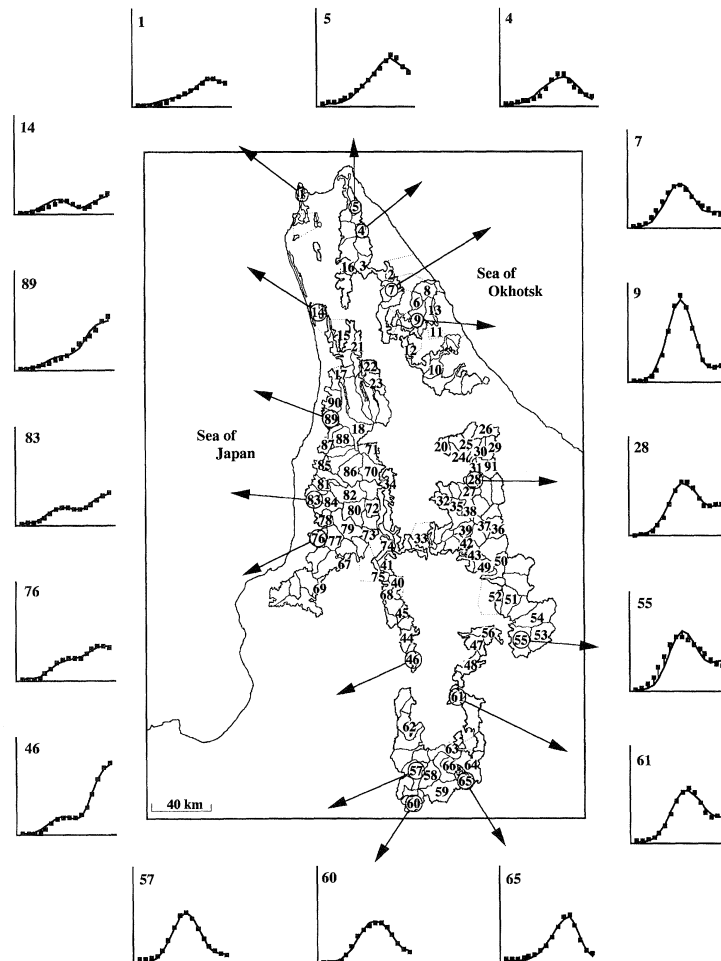

Figure 7. The map of the study area with a selection of spectral densities. The lines mark the border between the different ranger offices conducting the censuses. The 90 time series investigated are numbered (nos. 1–91; population no. 19 was incomplete and not part of the study). Reconstituted spectral densities (cf. figure 5) for a selection of the populations are given along the perimeter. The displayed reconstruction is based on the first three eigenvectors.

variability in the high frequency part of the spectrum. Negative row scores indicate the presence of annual or multiannual cyclicity. The second eigenvector represents the medium frequency part of the spectrum. Positive row scores indicate the presence of multiannual cyclicity. The dominant period corresponds to a 3.75 year cycle. Negative row scores indicate that the short term oscillatory component of the first eigenvector is dominating the dynamics. The third eigenvector operate as a modulator of the dominant period. The 3.75 cycle peak will be shifted to the right (shorter period) if the row score is positive, and to the left (longer period) if the row score is negative. This effect is easily seen when comparing the reconstituted data based on 2 or 3 eigenvectors (figure 5). Most of the variation is described by the first two eigenvectors. The additional calibration produced by the third may or may not be necessary.

A supplement to the biplot is to plot the row scores on a geographic map (figure 6). For the present data, the row scores exhibit strong spatial consistency for both the first and the second eigenvector. In particular, an opposition between the dynamics of the eastern and western populations is apparent. This enable us to conclude that the northeastern mountainous populations are generally characterized by multiannual cycles, whereas the western populations (close to the Sea of Japan) are dominated by short-term oscillations. The pattern is reminiscent of that of figure 2, but with far greater spatial consistency. The weak spatial consistency in the row scores accompanying the third eigenvector, may cast further doubt on its biological significance. A spatial map of the region studied, with a representative selection of observed and reconstituted spectral densities are given in figure 7. The difference between the eastern and the western populations is again marked. However, when examining closely the western populations these can been seen as being either biannually fluctuating (e.g. populations 46 and 89) or aperiodically fluctuating (populations 1, 14, 76, and 83). From inspecting all of the reconstitutions (not shown), it appears that two distinct areas are dominated by aperiodic fluctuations: the northwestern coastal area (populations 1, 14, 15, 16, and 21) and the western-central coastal part of the study area (populations 76, 77, 79, 83 and 84). The remainder of the western populations exhibit oscillations with a tendency towards a two year periodicity.

As already indicated, there is a general tendency for the eastern and more cyclic populations to be at a higher elevation. Hence, it is unclear whether altitude or the distance from the Sea of Japan (DSJ) is the best predictor of the row scores. The non-parametric regression reveal that the first row score (figure 4a) was significantly related to the DSJ and less so to the altitude (DSJ: d.f. = 1.1, $F = 16.9$, $p < 0.01$; altitude: d.f. = 1.2, $F = 5.71$, $p = 0.01$). The second row score (figure 4b) was also most related to DSJ (DSJ: d.f. = 1.1, $F = 20.2$, $p < 0.01$; altitude: d.f. = 1.2, $F = 1.84$, $p = 0.17$). The third row score (figure 4c) was related to neither the DSJ nor the altitude (DSJ: d.f. = 1.1, $F = 0.01$, $p = 0.95$; altitude: d.f. = 1.2, $F = 1.15$, $p = 0.74$). The latter corroborate

the previous doubt about the importance of the third row score.

4. DISCUSSION

(a) Methodology

To estimate the spectral densities we used the Parzen window with a width of 5. We have investigated the sensitivity of the results to this choice by using both wider and more narrow windows, as well as windows of different types (the Tukey-Hamming, the triangular and the uniform; Priestley 1981). The estimated spectral densities and the biogeographic patterns are very similar in all instances (O. N. Bjørnstad, S. Champely, N. Chr. Stenseth & T. Saitoh, unpublished data). In general, a very narrow window results in less clear pattern and less important eigenvectors. This can be interpreted as being due to the inconsistency of the periodogram as an estimator of the spectral density. A very wide window, on the other hand, results in over-smoothing of the pattern and a loss of detail. We chose to report the results for the window of width 5, because these results are representative and because this width is consistent with that recommended in the literature (Priestly 1981).

The results of the analysis clearly identifies the geographic pattern in the dynamics. It is interesting to note how much clearer the pattern is when the whole spectral density is considered (figure 6) as compared to that of the maximum period only (figure 2). Certainly, if one were to test for the significance of each univariate spectral density one may fail to appreciate the inherent cyclicity of some of the populations in the eastern region. We see how a classical multivariate approach can aid in identifying biogeographic patterns in population dynamics.

(b) Ecology

In this study we have documented the biogeographic pattern in the fluctuations of the grey-sided vole of the northernmost part of Hokkaido by using multivariate and graphical analyses of 90 populations. By analysing the time series in the frequency domain we have been able to decompose the time series in aperiodic or short-term oscillations and multiannual cycles. The period of the multiannual cycle, when observed, was typically 3.5–4 years. The geographic structure was conspicuous. Populations in the west of the study area (close to the Sea of Japan) do not exhibit multiannual cycles, whereas the eastern and interior populations do. The differences in dynamics appear to correlate more with distance from the Sea of Japan than with altitude as such. Both factors are considered to be epiphenomenlogical descriptors correlated with underlying unspecified biologically meaningful variables. Among the western populations, two seemingly distinct areas (one northern and one more central) exhibit aperiodic dynamics, the remaining areas entertain variable degrees of two year periodicity.

Both periodic and non-periodic fluctuations are commonly reported in microtines (Hansson & Hent-

tonen 1985; Hanski *et al.* 1991; Stenseth & Ims 1993). A classical interpretation of the aperiodic fluctuations is that the underlying dynamics are stable, but with stochasticities superimposed (the 'semi-stable' dynamics of Hansson & Henttonen 1985; see also Hansson 1971). The stochasticity may include both demographic and seasonal variation.

Recently, it has been suggested that seemingly aperiodic fluctuations in population abundances may be due to nonlinearities and chaotic dynamics (e.g. May 1987). This alternative has been the focus of many recent studies on microtine population dynamics (e.g. Hanski & Korpimäki 1995; see also Falck *et al.* 1995*a,b*). This issue cannot be resolved by spectral analysis. However, an investigation of the degree of nonlinearity in these time series has revealed that the actual nonlinearities, if any, are weak (Stenseth *et al.* 1996). The available information, thus, suggests a role for stochasticity.

Population dynamic clines, like the gradient observed in Hokkaido from the western coast towards the East and mountainous interior, represent important ecological insights. Our results provide a new example of how important dynamic characteristics can vary biogeographically. The basic assumption that essentially similar mechanisms operate in large parts of a species distribution underlies out work, as it does that of many other researchers. The relative importance of different processes may vary at a large scale, though, to produce one type of dynamics in one region and a different type in another.

In the phenomenologically similar Fennoscandian transition to cyclicity, several hypotheses have been put forward (see, for example, Bjørnstad *et al.* 1995). These may be of use as a point of departure for investigating the pattern documented above. The most influential hypotheses pertain to snow cover (e.g. Hansson & Henttonen 1985; Hansson 1987), and predation (e.g. Hansson & Henttonen 1988; Hanski *et al.* 1991). Seasonality, more generally, has also been considered (e.g. Hanski & Korpimäki 1995). The hypotheses are, largely, centred around the ability of specialist predators to generate predator–prey abundance cycles. An otherwise stable microtine population may undergo cycles in the presence of mustelid predators (present in Fennoscandia as well as in Hokkaido). The abundance, density and diversity of generalist predators are thought to modulate the periodicity of such an interaction to generate the Fennoscandian gradient in dynamics (Hanski *et al.* 1991). Seasonality may play a direct role by determining the length of the breeding season. Seasonality will also, together with other climatic forces, determine the depth and duration of snow cover.

From the row scores we see that the multiannual cycles occur in the area with overall longer duration of snow cover. At present, the data we have are too coarse and too scarce to give detailed geographic information on the distribution and abundance of predators; so further speculation must await the results of future studies. The proximate causes of mortality in microtine populations appear to be a key to understanding small rodent population dynamics (Norrdahl & Korpimäki

1995; Reid *et al.* 1995; Steen 1995). On the basis of our results we recommend that an investigation of differences in mortality among the grey-sided vole populations of Hokkaido is among the issues given priority.

Similar gradients to those observed in Fennoscandia and Hokkaido have not been documented elsewhere. Either, the two regions represent rather unique systems, or geographic patterns may not be uncommon, but remain undiscovered due to too little data and/or inappropriate methodology.

REFERENCES

Bjørnstad, O. N., Falck, W. & Stenseth, N. C. 1995 Geographic gradients in population dynamics of microtine rodents: statistical evidence of changing patterns of density dependence. *Proc. R. Soc. Lond.* B **262**, 127–133.

Bulmer, M. G. 1974 A statistical analysis of the 10-year cycle in Canada. *J. Anim. Ecol.* **43**, 701–18.

Castro, P. E., Lawton, W. H. & Sylvestre, E. A. 1986 Principal modes of variation for processes with continuous sample curves. *Technometrics* **28**, 329–337.

Chessel, D. & Dolédec, S. 1992 *ADE*: *HyperCard* © Stacks and programme library for the analysis of environmental data (*Ver.* 3.7), URA CNRS 1451, Université Lyon 1, 69622 Villeurbanne cedex.

Colebrook, J. M. 1978 Continuos plankton records: zooplankton and environment, North-East Atlantic and North Sea, 1948–1975. *Oceanol. Acta* **1**, 9–23.

Danell, K. 1985 Population fluctuations of the muskrat in coastal northern Sweden. *Acta Theriol.* **30**, 219–227.

Dobson, M. 1994 Patterns of distribution in Japanese land mammals. *Mamm. Rev.* **24**, 91–111.

Eckart, C. & Young, G. 1936 The approximation of one matrix by another of lower rank. *Psychometrika* **1**, 211–218.

Elton, C. & Nicholson, M. 1942 Fluctuations in numbers of the muskrat (*Ondatra zibethica*) in Canada. *J. Anim. Ecol.* **11**, 96–126.

Falck, W., Bjørnstad, O. N. & Stenseth, N. C. 1995*a* Bootstrap estimated uncertainty of the dominant Lyapunov exponent for Holarctic microtine rodents. *Proc. R. Soc. Lond.* B **261**, 159–165.

Falck, W., Bjørnstad, O. N. & Stenseth, N. C. 1995*b* Voles and lemmings – chaos and uncertainty in fluctuating populations. *Proc. R. Soc. Lond.* B **262**, 363–370.

Gabriel, K. R. 1971 The biplot graphical display of matrices with application to principal component analysis. *Biometrika* **58**, 453–467.

Gilbert, B. S. & Krebs, C. J. 1991 Population dynamics of *Clethrionomys* and *Peromyscus* in southwestern Yukon 1973–1989. *Holarct. Ecol.* **14**, 250–259.

Goodall, D. W. 1954 Objective methods for the classification of vegetation III. An essay in the use of factor analysis. *Austr. J. Bot.* **2**, 304–324.

Hanski, I., Hansson, L. & Henttonen, H. 1991 Specialist predators, generalist predators, and the microtine rodent cycle. *J. Anim. Ecol.* **60**, 353–367.

Hanski, I., Henttonen, H. & Hansson, L. 1994 Temporal variability and geographical patterns in the population density of microtine rodents: A reply to Xia and Boonstra. *Am. Nat.* **144**, 329–342.

Hanski, I. & Korpimäki, E. 1995 Microtine rodent dynamics in northern Europe: Parametrized models for the predator-prey interaction. *Ecology* **76**, 840–850.

Hansson, L. 1971 Habitat, food and population dynamics of the field vole *Microtus agrestis* (L.) in South Sweden. *Viltrevy Swed. Wildl.* **8**, 267–378.

Hansson, L. 1987 An interpretation of rodent dynamics as due to trophic interactions. *Oikos* **50**, 308–318.

Hansson, L. & Henttonen, H. 1985 Gradients in density variations of small rodents: the importance of latitude snow cover. *Oecologia* **67**, 394–402.

Hansson, L. & Henttonen, H. 1988 Rodent dynamics as community processes. *Trend. Ecol. Evol.* **3**, 195–200.

Hastie, T. & Tibshirani, R. 1990 *Generalized additive models.* London: Chapman and Hall.

Henttonen, H., McGuire, D. & Hansson, L. 1985 Comparisons of amplitude and frequencies (spectral analyses) of density variations in long-term data sets of *Clethrionomys* species. *Ann. Zool. Fenn.* **22**, 221–27.

Henttonen, H., Hansson, L. & Saitoh, T. 1992 Rodent dynamics and community structure: *Clethrionomys rufocanus* in northern Fennoscandia and Hokkaido. *Ann. Zool. Fenn.* **29**, 1–6.

Jackson, J. E. 1986 *A user's guide to principal components.* New York: Wiley.

May, R. M. 1987 Chaos and the dynamics of biological populations. *Proc. R. Soc. Lond.* A **413**, 27–44.

Nakata, K. 1989 Regulation of reproductive rate in a cyclic population of the red-backed vole, *Clethrionomys rufocanus bedfordiae. Res. Popul. Ecol.* **31**, 185–209.

Norrdahl, K. & Korpimäki, E. 1995 Mortality factors in a cyclic vole population. *Proc. R. Soc. Lond.* B **261**, 49–53.

Priestley, M. B. 1981 *Spectral analysis and time series.* London: Academic Press.

Reid, D. G., Krebs, C. J. & Kenney, A. 1995 Limitation of collard lemming population growth at low densities by predation mortality. *Oikos* **73**, 387–398.

Royama, T. 1992 *Analytical population dynamics.* London: Chapman & Hall.

Saitoh, T. 1987 A time series and geographical analysis of population dynamics of the red-backed vole in Hokkaido, Japan. *Oecologia* **73**, 382–388.

Saitoh, T. 1991 The effects and limits of territoriality on population regulation in grey red-backed voles, *Clethrionomys rufocanus bedfordiae. Res. Popul. Ecol.* **33**, 367–386.

Saitoh, T., Bjørnstad, O. N. & Stenseth, N. C. 1996 Density Dependence in Grey-sided Vole Populations. *J. Anim. Ecol.* (In the press.)

SAS Institute. 1990 *SAS/ETS user guide, version 6,* edn 4. Cary, North Carolina: SAS Institute Inc.

Statistical Sciences, I. 1993 *S-plus for windows version 3.2 supplement.* Seattle: Statistical Sciences Inc.

Steen, H. 1995 Untangling the causes of disappearance from a local population of root voles, *Microtus oeconomus*: a test for the regional synchrony hypothesis. *Oikos* **73**, 65–72.

Stenseth, N. C. & Ims, R. A. 1993 *The biology of lemmings.* London: Academic Press.

Stenseth, N. C., Bjørnstad, O. N. & Saitoh, T. 1996 A gradient from stable to cyclic populations of *Clethrionomys rufocanus* in Hokkaido, Japan. (Submitted.)

Tatewaki, M. 1958 Forest ecology of the islands of the north pacific ocean. *J. Fac. Agric. Hokk. Univ.* **50**, 371–472.

Upton, G. J. G. & Fingleton, B. 1985 *Spatial data analysis by example, vol.* 1. *Point pattern and quantitative data.* Chichester: Wiley.

Wei, W. W. 1989 *Time series analysis.* California: Addison Wesley.

Wilson, D. E. & Reeder, D. A. (eds) 1993 *Mammal species of the world,* edn 2. Washington: Smithsonian Institution Press.